Peng, S.-M., & Ibers, J. A. (1976) *J. Am. Chem. Soc. 98*, 8032-8036.
Phillips, S. E. V. (1980) *J. Mol. Biol. 142*, 531-554.
Phillips, S. E. V., & Schoenborn, B. P. (1981) *Nature 292*, 81-82.
Satterlee, J. D. (1985) *Annu. Rep. NMR Spectrosc. 17*, 80-178.
Scheidt, W. R., Ja Lee, Y., Luangdilok, W., Haller, K. J., Anzai, K., & Hatano, K. (1983) *Inorg. Chem. 22*, 1516-1522.
Shulman, R. G., Glarum, S. H., & Karplus, M. (1971) *J. Mol. Biol. 57*, 93-115.
Springer, B. A., Egeberg, K. D., Sligar, S. G., Rohlfs, R. J., Mathews, A. J., & Olson, J. S. (1989) *J. Biol. Chem. 264*, 3057-3060.
Steigemann, W., & Weber, E. (1979) *J. Mol. Biol. 127*, 309-336.
Takano, T. (1977) *J. Mol. Biol. 110*, 537-568.
Traylor, T. G., & Berzinis, A. P. (1980) *J. Am. Chem. Soc. 102*, 2844-2846.
Williams, G., Clayden, N. J., Moore, G. R., & Williams, R. J. P. (1985) *J. Mol. Biol. 183*, 447-460.
Wüthrich, K. (1970) *Struct. Bonding 8*, 53-121.
Wüthrich, K., Shulman, R. G., Yamane, T., Wyluda, B. J., Hügli, T. E., & Gurd, F. R. N. (1970) *J. Biol. Chem. 245*, 1947-1953.

Studies on the Solution Conformation of Human Thioredoxin Using Heteronuclear ^{15}N-^{1}H Nuclear Magnetic Resonance Spectroscopy†

Julie D. Forman-Kay,‡,§ Angela M. Gronenborn,*,‡ Lewis E. Kay,‡ Paul T. Wingfield,∥,⊥ and G. Marius Clore*,‡

Laboratory of Chemical Physics, Building 2, National Institute of Diabetes and Digestive and Kidney Diseases, National Institutes of Health, Bethesda, Maryland 20892, Department of Molecular Biophysics and Biochemistry, Yale University, New Haven, Connecticut 06511, and Glaxo Institute for Molecular Biology SA, 46 Route des Acacias, CH-1211 Geneva, Switzerland

Received August 2, 1989; Revised Manuscript Received September 28, 1989

ABSTRACT: The solution conformation of uniformly labeled ^{15}N human thioredoxin has been studied by two-dimensional heteronuclear ^{15}N-^{1}H nuclear magnetic resonance spectroscopy. Assignments of the ^{15}N resonances of the protein are obtained in a sequential manner using heteronuclear multiple quantum coherence (HMQC), relayed HMQC-correlated (COSY), and relayed HMQC-nuclear Overhauser (NOESY) spectroscopy. Values of the $^{3}J_{HN\alpha}$ splittings for 87 of the 105 residues of thioredoxin are extracted from a variant of the HMQC-COSY experiment, known as HMQC-*J*, and analyzed to give accurate $^{3}J_{HN\alpha}$ coupling constants. In addition, long-range $C_{\alpha}H(i)$-$^{15}N(i+1)$ scalar connectivities are identified by heteronuclear multiple bond correlation (HMBC) spectroscopy. The presence of these three-bond scalar connectivities in predominantly α-helical regions correlates well with the secondary structure determined previously from a qualitative analysis of homonuclear nuclear Overhauser data [Forman-Kay, J. D., Clore, G. M., Driscoll, P. C., Wingfield, P. T., Richards, F. M., & Gronenborn, A. M. (1989) *Biochemistry 28*, 7088-7097], suggesting that this technique may provide additional information for secondary structure determination a priori. The accuracy with which $^{3}J_{HN\alpha}$ coupling constants can be obtained from the HMQC-*J* experiment permits a more precise delineation of the beginnings and ends of secondary structural elements of human thioredoxin and of irregularities in these elements.

The application of nuclear magnetic resonance (NMR)[1] spectroscopy to the determination of three-dimensional structures of proteins in solution has advanced rapidly in the past few years [see Wüthrich (1986) and Clore and Gronenborn (1987, 1989) for reviews]. A formidable limitation, however, still exists with respect to the size of molecules to which the methodology can be applied. One avenue for resolving ambiguities in assignment arising from severe spectral overlap associated with molecules larger than ~10 kDa was opened by the development of heteronuclear ^{15}N-^{1}H experiments. In addition to the powerful three-dimensional heteronuclear experiments reported recently (Marion et al., 1989a,b; Zuiderweg & Fesik, 1989), two-dimensional heteronuclear relayed multiple quantum and multiple bond correlation experiments can also be used to deal with problems caused by overlapping resonances and confirm assignments (Gronenborn et al., 1989a,b; Clore et al., 1988). ^{15}N-^{1}H HMQC, relayed HMQC-NOESY, HMQC-COSY, and HMBC experiments have been recorded on human thioredoxin

†This work was supported by the Intramural AIDS Targeted Antiviral Program of the Office of the Director, NIH (A.M.G. and G.M.C.). J.D.F. acknowledges a graduate fellowship from the Molecular Biophysics and Biochemistry Department of Yale University and support from NIH Grant GM-22778 (to F. M. Richards, Yale University).

‡National Institutes of Health.
§Yale University.
∥Glaxo Institute for Molecular Biology SA.
⊥Present address: Protein Expression Laboratory, Building 6B, National Institutes of Health, Bethesda, MD 20892.

[1] Abbreviations: NMR, nuclear magnetic resonance; HMQC, heteronuclear multiple quantum correlation spectroscopy; NOESY, two-dimensional nuclear Overhauser effect spectroscopy; COSY, two-dimensional correlated spectroscopy; HMQC-COSY, relayed heteronuclear multiple quantum coherence correlated spectroscopy; HMQC-NOESY, relayed heteronuclear multiple quantum coherence nuclear Overhauser spectroscopy; HMBC, heteronuclear multiple bond correlation spectroscopy; NOE, nuclear Overhauser effect; *E. coli*, *Escherichia coli*; DTT, dithiothreitol.

0006-2960/90/0429-1566$02.50/0

to obtain accurate $^3J_{HN\alpha}$ coupling constants, to confirm the previous proton resonance assignments and secondary structure determination derived from purely homonuclear methods (Forman-Kay et al., 1989), and to remove ambiguities in the assignment of the long-range NOE peaks. The excellent correlation of the NMR parameters with the secondary structure, augmented by accurate coupling constant data, allows a finer determination of the beginnings and ends of the α-helices and β-strands in human thioredoxin and yields specific information regarding irregularities in these secondary structural elements.

Experimental Procedures

Human thioredoxin was purified from a strain of *E. coli* containing a temperature-sensitive repressor and a plasmid bearing the thioredoxin gene under the control of the λ P_l promoter and phage Mu *ner* gene ribosome binding site, as described in Wollman et al. (1988). The bacteria were grown in minimal medium using $^{15}NH_4Cl$ as the sole nitrogen source to achieve essentially complete ^{15}N labeling of the protein. Two species of thioredoxin differing in the presence or absence of the N-terminal methionine were produced due to inefficient posttranslational processing, with the ratio 30% N-Met/70% N-Val as determined by N-terminal amino acid sequencing. For NMR samples, 2 mM protein was reduced with excess dithiothreitol (DTT), dialyzed against 150 mM phosphate buffer, pH 5.5, containing 0.2 mM DTT, lyophilized, redissolved in argon-purged 99.996% D_2O or 90% H_2O/10% D_2O, sealed in tubes with airtight rubber septa, and blanketed with argon for 30 min.

All experiments were recorded on a Bruker AM600 spectrometer at 40 °C and were processed on an ASPECT 3000 computer. Quadrature in F_1 was obtained by using the time proportional phase incrementation method (Marion & Wüthrich, 1983). The ^1H detected heteronuclear multiple quantum correlation (HMQC) experiment (Bax et al., 1983; Bendell et al., 1983) and the relayed HMQC-correlated (HMQC-COSY) and HMQC-nuclear Overhauser effect (HMQC-NOESY) experiments (Gronenborn et al., 1989a) were recorded in H_2O, collecting 256 or 512 t_1 increments of 2K data points. To measure $^3J_{HN\alpha}$ coupling constants, a variant of the HMQC-COSY experiment, known as HMQC-*J* (Kay & Bax, 1990), was recorded using the pulse scheme

^1H: $90°_x$ - τ - - $t_1/2$ - $180°_\alpha$ - $t_1/2$ - - τ - $90°_y$ - Acq

^{15}N: $90°_\beta$ $90°_\delta$ Decoupling

with phase cycling $\alpha = 2(x)\ 2(y)\ 2(-x)\ 2(-y)$; $\beta = x, -x$; $\delta = 8(x)\ 8(-x)$; and Acq = $2(x, -x, -x, x)\ 2(-x, x, x, -x)$. The delay τ was set to 4.5 ms, slightly less than $1/(2J_{NH})$. This experiment was also recorded in H_2O with 1248 t_1 increments of 2K data points to give an acquisition time in t_1 of 250 ms. Zero-filling in F_1 gave a final digital resolution of 0.5 Hz/point in the ^{15}N dimension. The pulse sequence and phase cycling for the HMQC-*J* experiment (Kay & Bax, 1990) are identical with that of the HMQC-COSY experiment (Gronenborn et al., 1989a) and differ from the normal HMQC experiment by the addition of a ^1H $90°_y$ pulse immediately before acquisition. This suppresses the dispersive contributions to the line shape in F_2. For all experiments in H_2O, water suppression was achieved with coherent presaturation. The heteronuclear multiple bond correlation (HMBC) experiment (Bax & Summers, 1986; Clore et al., 1988) was carried out in D_2O with 256 t_1 increments of 1K data points. The HMBC spectrum was recorded in mixed mode, with pure phase absorption in the ^{15}N F_1 dimension and absolute value in the ^1H F_2 dimension (Bax & Marion, 1988).

Results and Discussion

Assignment of the ^{15}N resonances in combination with a variety of heteronuclear experiments can confirm and add structurally relevant data about a protein to that already obtained from homonuclear results. Although essentially complete ^1H assignments of human thioredoxin could be obtained by using purely homonuclear methods because of the relatively large chemical shift dispersion (Forman-Kay et al., 1989), information from ^{15}N-^1H spectra was extracted to augment the available data. The relayed HMQC-NOESY (Figures 1A and 2A) and HMQC-COSY (Figure 1B) spectra contain essentially the same information as the NH region of their homonuclear counterparts, except that the NH ^1H chemical shift axis is replaced by the ^{15}N chemical shift axis. ^{15}N sequential assignment proceeds in an analogous manner to the ^1H sequential assignment. Direct and relayed scalar connectivities from the ^{15}N atom to the intraresidue NH and $C_\alpha H$ atoms are obtained from the HMQC and HMQC-COSY spectra, respectively. Sequential through-space NOE connectivities involving the NH protons are relayed to the corresponding ^{15}N atom and identified in the HMQC-NOESY spectrum. Since the ^{15}N assignment could be done in a manner independent of the NH assignments, it offered a useful check of the previously determined ^1H chemical shifts (Forman-Kay et al., 1989). In addition, the ^{15}N assignment aided the resolution of ambiguities in the assignment of long-range NOEs necessary for a complete tertiary structure determination, since chemical shift degeneracy or near degeneracy of particular NH proton resonances is generally not present for the corresponding ^{15}N resonances and vice versa. Table I lists the ^{15}N chemical shifts for resonances from both forms of human thioredoxin, the minor species containing the N-terminal methionine and the major species lacking this residue, leaving an N-terminal valine. Resonances with distinguishable NH or $C_\alpha H$ ^1H chemical shifts for the two forms are denoted with an asterisk on the amino acid name of the resonance arising from the major N-Val species.

Apparent $^3J_{HN\alpha}$ splittings were measured directly from F_1 cross sections of the HMQC-*J* spectrum (Figure 2B). These measured values do not represent the actual couplings since the line shape of the multiplets is not purely absorptive and because the two peaks of the multiplet overlap. The dispersive component of the line shape leads to overestimation of the $^3J_{HN\alpha}$ value for large couplings, and the multiplet overlap causes underestimation and even disappearance of the splittings for small couplings. Figure 3A displays the apparent $^3J_{HN\alpha}$ splittings as a function of the true $^3J_{HN\alpha}$ coupling constants and illustrates the effect of dispersive line-shape components and finite line widths on the apparent $^3J_{HN\alpha}$ splittings. The curves were generated by extracting the maxima from line shapes simulated by the Fourier transformation of a function describing the t_1 evolution of magnetization for the HMQC-*J* sequence, modified by the application of a Gaussian apodization function. The time domain response for a multiplet centered at zero frequency is given by the expression $\cos(2\pi^3 J_{HN\alpha}\tau + t_1)e^{-t_1/T_{2,MQ}}$, where $T_{2,MQ}$ refers to the multiple quantum relaxation time and τ is the delay time that allows for efficient creation of heteronuclear multiple quantum coherence [in this case τ was set to 4.5 ms, slightly less than $1/(2J_{NH})$]. The multiple quantum line width was assumed to be 10 Hz, and four different line-broadening parameters of the Gaussian apodization function were used, as indicated in Figure 3A.

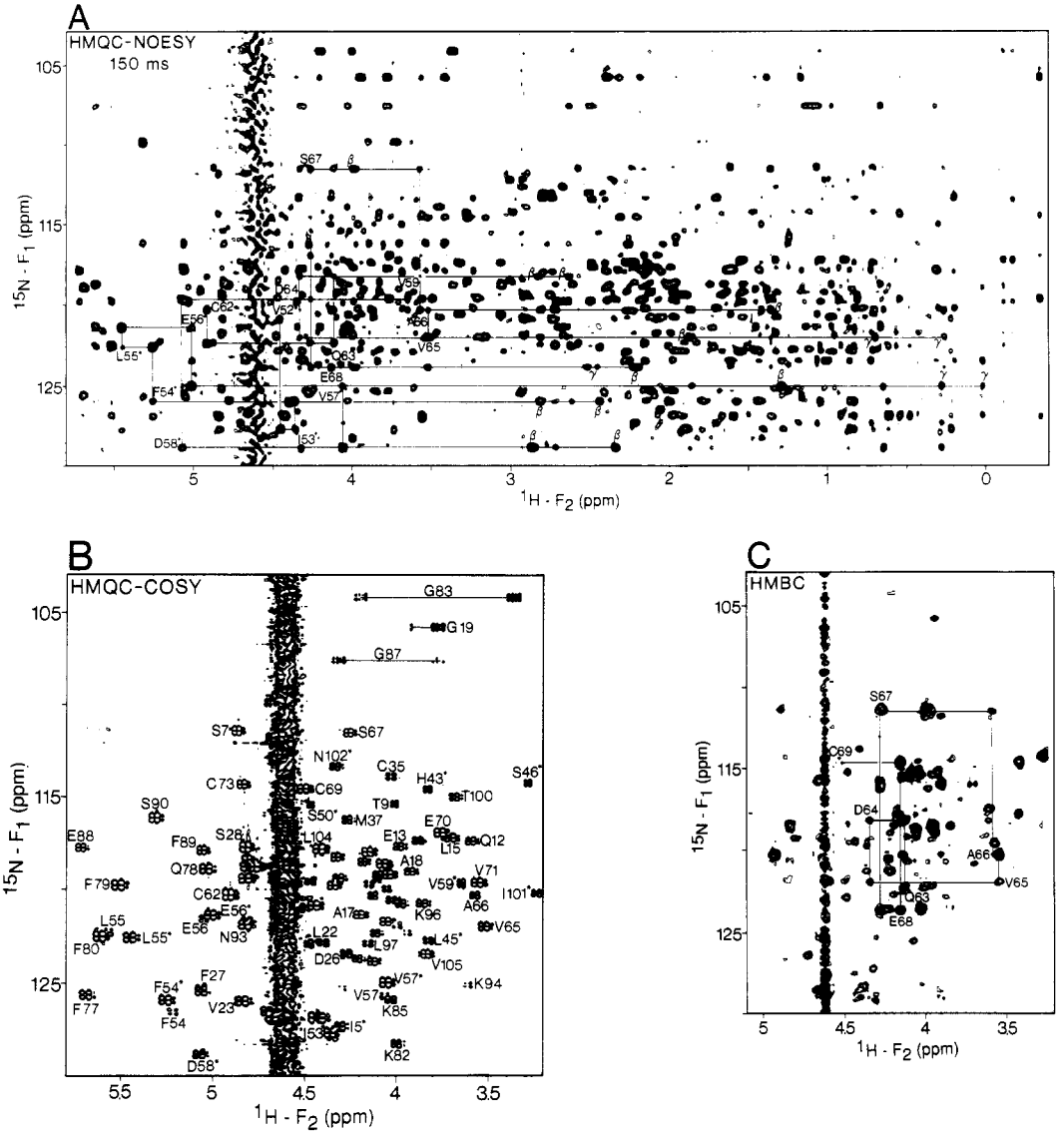

FIGURE 1: ^{15}N (F_1 axis)–aliphatic ^{1}H (F_2 axis) region of the 150-ms relayed ^{15}N–^{1}H HMQC–NOESY spectrum in H_2O (A), the ^{15}N (F_1 axis)–$C_\alpha H$ ^{1}H (F_2 axis) region of the relayed ^{15}N–^{1}H HMQC–COSY spectrum in H_2O (B), and the ^{15}N (F_1 axis)–$C_\alpha H$ ^{1}H (F_2 axis) region of the HMBC spectrum in D_2O (C) of ^{15}N-labeled reduced recombinant human thioredoxin (30% N-Met/70% N-Val) at 40 °C and pH 5.5. In the HMQC–NOESY spectrum (A) selected $C_\alpha H(i)$–^{15}N(i+1) from residue Val-52* to residue Val-59* and from Cys-62 to Glu-68 are indicated. In the HMBC spectrum (C), selected $C_\alpha H(i)$–^{15}N(i+1) connectivities are also indicated. Peaks with distinguishable chemical shifts between the two forms and arising from the major N-terminal Val species are denoted with an asterisk.

To correct the experimentally measured $^3J_{HN\alpha}$ values for the errors demonstrated in Figure 3A, the following strategy was employed. The HMQC–J spectrum was processed with a Gaussian apodization function in F_1 using four different negative line-broadening parameters (−4, −6, −8, and −10 Hz) and a curve with a maximum at the end of the t_1 time domain data to optimize resolution. Processing the data with at least two different negative line-broadening parameters is required to extract $^3J_{HN\alpha}$ and line-width values from each multiplet. In practice, more accurate $^3J_{HN\alpha}$ values can be obtained by using estimated splittings based on three or more line-broadening parameters. Splittings measured from experimental spectra processed with the different parameters, along with initial guesses of the true $^3J_{HN\alpha}$ values and multiple quantum line widths, were entered into a least-squares minimization program. Corrected values of $^3J_{HN\alpha}$ were obtained by varying the input values of $^3J_{HN\alpha}$ and the multiple quantum line widths using Powell's nonlinear optimization algorithm (Powell, 1965) to minimize the differences between the measured values of $^3J_{HN\alpha}$ for the different values of the line-broadening parameter and the corresponding calculated values of the apparent $^3J_{HN\alpha}$ splittings obtained from the line-shape simulated as described above. The corrected values of the $^3J_{HN\alpha}$ coupling constants are presented in Table I.

The significantly narrower multiple quantum line widths in the F_1 dimension (Bax et al., 1989), coupled with the analysis described above which corrects for multiple quantum line widths and dispersive contributions, result in $^3J_{HN\alpha}$ values whose accuracy far exceeds that of the apparent coupling constants measured directly from homonuclear COSY-type experiments without correction for the broad homonuclear NH line widths. This latter technique results in substantial overestimation in the values of the coupling constants unless similar methods for correcting the $^3J_{HN\alpha}$ values to that used here are employed. A fundamental limitation, however, of the homonuclear COSY experiment is that the minimum separation of the anti phase components of the NH–$C_\alpha H$ COSY cross-peaks is approximately half the NH line width (Neuhaus et al., 1985). Typical homonuclear NH line widths for proteins the size of thioredoxin are between 10 and 20 Hz, making it impossible to measure many couplings in α-helical regions, which normally lie between 3 and 6 Hz. The lower limit for

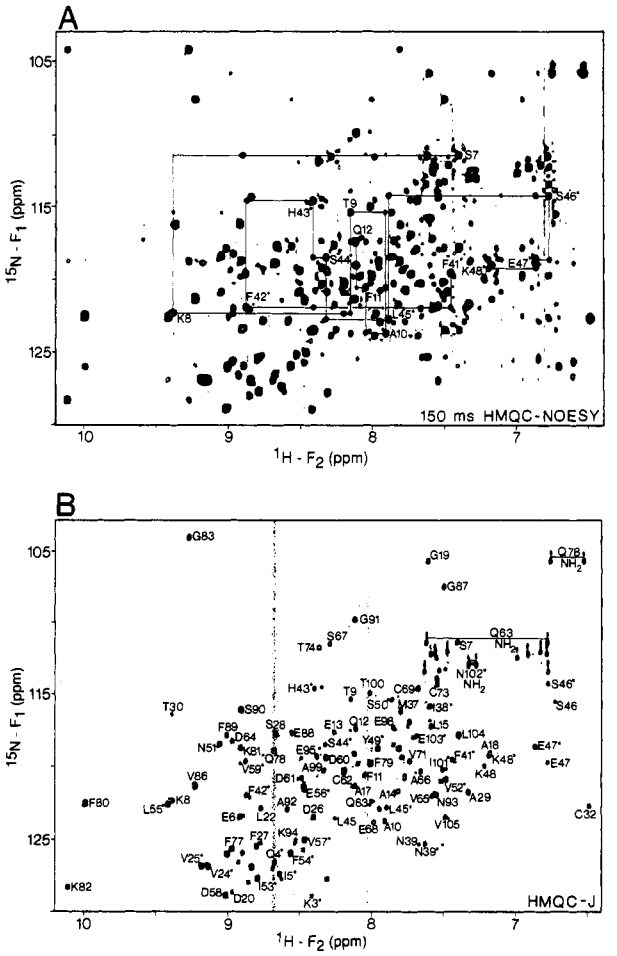

FIGURE 2: ^{15}N (F_1 axis)–NH/aromatic ^{1}H (F_2 axis) region of the 150-ms relayed ^{15}N–^{1}H HMQC–NOESY spectrum (A) and the HMQC–J spectrum (B) of ^{15}N-labeled reduced recombinant human thioredoxin (30% N-Met/70% N-Val) at 40 °C and pH 5.5. In the HMQC–NOESY spectrum (A) selected ^{15}N(i)–NH(i+1) connectivities from residue Ser-7 to residue Gln-12 and from Phe-41* to Lys-48* are indicated. Peaks with distinguishable chemical shifts between the two forms and arising from the major N-terminal Val species are denoted with an asterisk.

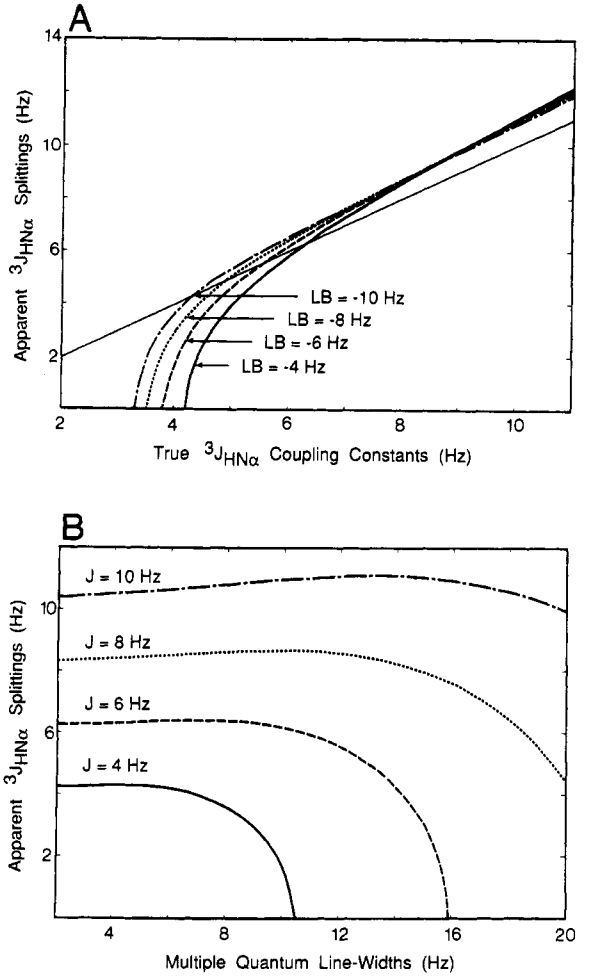

FIGURE 3: (A) Apparent $^3J_{HN\alpha}$ splittings extracted from line shapes simulated by Fourier transformation of the t_1 time domain response, plotted as a function of the true $^3J_{HN\alpha}$ value for different negative line-broadening values (LB) of the Gaussian apodization function of −10 Hz (- - -), −8 Hz (···), −6 Hz (---), and −4 Hz (—), assuming a multiple quantum line width of 10 Hz. Note that the Gaussian curve used has a maximum at the end of the time domain (i.e., GB = 1). To guide the eye, a straight line given by $^3J_{HN\alpha}$(apparent) = $^3J_{HN\alpha}$(true) is also drawn. (B) Apparent $^3J_{HN\alpha}$ splittings as a function of multiple quantum line width, for values of the true $^3J_{HN\alpha}$ coupling of 4 Hz (—), 6 Hz (---), 8 Hz (···), and 10 Hz (- - -), assuming LB = −6 Hz and GB = 1.

measurable couplings in the HMQC–J experiment is well below that of the COSY experiments due to the intrinsically narrower multiple quantum line widths. The smallest apparent splittings measured in the HMQC–J spectrum of human thioredoxin were 2.0 Hz with corrected $^3J_{HN\alpha}$ values of 3.8 and 4.0 Hz for Asp-102* and Lys-94, respectively.

To estimate the precision of the corrected values of the $^3J_{HN\alpha}$ coupling constants and to ensure that the values derived from the least-squares fitting procedure were not in local minima, different initial guesses for the line width and $^3J_{HN\alpha}$ values were used as input. Values of $^3J_{HN\alpha}$ varying within ±0.5 Hz for large couplings and within ±1.0 Hz for small couplings were obtained for different initial guesses. Large couplings seem to be more robust to experimental errors in measuring the $^3J_{HN\alpha}$ splittings since there is less of a dependence on the multiple quantum line width, as indicated in Figure 3B. Within the 10–14-Hz regime, where the multiple quantum line widths of human thioredoxin at 40 °C lie, this dependence is only significant for $^3J_{HN\alpha}$ values less than 6 Hz. The accuracy of these small $^3J_{HN\alpha}$ values, nevertheless, is still extremely good. In addition, only four $^3J_{HN\alpha}$ splittings in the HMQC–J spectrum of human thioredoxin were too small to be measured, namely, those for Thr-9, Gln-12, Thr-30, and Asn-39.

The $^3J_{HN\alpha}$ values determined by using the HMQC–J experiment and subsequent numerical analysis correlate well with the secondary structure determined from a qualitative interpretation of homonuclear NOESY patterns, NH exchange data, and the COSY-derived couplings. The structure of human thioredoxin elucidated from the previous homonuclear experiments and supported by these accurate $^3J_{HN\alpha}$ couplings is a mixed five-stranded β-sheet and four α-helices (Forman-Kay et al., 1989). The couplings measured are related to the ϕ torsion angle of the peptide backbone by a Karplus-like relationship (Karplus, 1963; Pardi et al., 1984). Values obtained for human thioredoxin are generally less than 6 Hz for α-helical regions and greater than 7 Hz for β-sheet regions. This contrasts with the data from the COSY experiment, where apparent couplings could only be categorized into ranges of less than 9 Hz for α-helical regions and greater than 9 Hz for regions of β-sheet (Forman-Kay et al., 1989). Figure 4 illustrates the correlation between the $^3J_{HN\alpha}$ coupling constants derived from the HMQC–J spectrum (Figure 4A) and the secondary structure of human thioredoxin (Figure 4C).

The secondary structure of human thioredoxin which was determined on the basis of homonuclear NOEs and COSY-derived splittings can also now be reevaluated by using information inherent in the accurate $^3J_{HN\alpha}$ splittings obtained

Table I: ^{15}N Assignments and $^3J_{HN\alpha}$ Coupling Constants for the N-Met and N-Val* Forms of Human Thioredoxin[a]

residue	^{15}N (ppm)	$^3J_{HN\alpha}$ (Hz)	residue	^{15}N (ppm)	$^3J_{HN\alpha}$ (Hz)	residue	^{15}N (ppm)	$^3J_{HN\alpha}$ (Hz)
M1	*b*	*b*	P40	129.1	*d*	E68	123.8	5.0
V2	*b*	*b*	F41*	119.5	6.5	C69	114.5	8.5
K3*	128.9	9.7	F41	119.7	*e*	E70	116.9	6.9
Q4*	126.5	6.9	F42*	121.9	4.8	V71	119.6	7.0
Q4	126.9	*e*	F42	122.1	4.4	K72	126.9	11.7
Q4 NH_2	112.3	*f*	H43*	114.6	4.8	C73	114.3	6.5
I5*	127.3	7.3	H43	114.4	*e*	T74	112.2	*e*
I5	127.7	*e*	S44*	118.4	5.4	P75	*d*	*d*
E6	123.4	7.6	S44	119.4	4.7	T76	119.0	7.1
S7	111.4	6.3	L45*	122.7	4.1	F77	125.6	9.7
K8	122.3	4.3	L45	123.4	4.7	Q78	118.8	10.8
T9	115.3	*g*	S46*	114.2	4.4	Q78 NH_2	105.8	*f*
A10	123.7	5.4	S46	115.5	4.4	F79	119.7	10.5
F11	120.5	4.4	E47*	118.5	7.2	F80	122.5	9.5
Q12	117.3	*g*	E47	119.7	*e*	K81	118.7	7.9
Q12 NH_2	113.4	*f*	K48*	119.2	7.5	K82	128.3	6.2
E13	117.6	4.4	K48	119.9	6.9	G83	104.2	5.6
A14	121.7	5.1	Y49*	118.7	8.9	Q84	118.7	9.7
L15	117.2	5.1	Y49	118.4	*e*	Q84 NH_2	112.1	*f*
D16	119.7	4.9	S50*	115.4	4.8	K85	125.9	5.4
A17	121.3	5.9	N51	118.3	8.2	V86	120.3	10.0
A18	119.0	4.7	N51 NH_2	112.2	*f*	G87	107.6	4.7
G19	105.8	5.7	V52*	120.7	9.8	E88	117.7	6.2
D20	128.5	*h*	V52	120.9	10.1	F89	117.8	5.6
K21	119.3	5.9	I53*	127.7	9.4	S90	116.1	8.5
L22	122.8	5.4	I53	127.9	*e*	G91	107.8	4.9
V23	126.0	10.0	F54*	125.9	9.7	A92	122.9	6.5
V24*	126.9	9.6	F54	126.6	*e*	N93	121.8	7.0
V24	126.8	*h*	L55*	122.6	9.7	N93 NH_2	112.6	*f*
V25*	126.8	9.7	L55	122.2	*e*	K94	125.1	4.0
V25	126.7	*h*	E56*	121.5	9.8	E95	119.2	5.3
D26	123.5	8.8	E56	121.3	*e*	K96	120.7	*h*
F27	125.4	9.1	V57*	125.0	10.1	L97	122.8	4.1
S28	117.7	8.5	V57	125.7	*e*	E98	117.3	4.9
A29	121.7	*e*	D58*	128.8	6.5	A99	120.3	4.2
T30	116.2	*g*	V59*	119.6	4.0	T100	115.0	5.5
W31	*b*	*b*	V59	119.8	4.8	I101*	120.2	4.8
C32	122.6	*e*	D60	119.4	8.6	N102*	113.3	3.8
G33	*c*	*c*	D61	120.8	6.8	N102	113.2	4.7
P34	128.8	*d*	C62	120.3	9.9	N102 NH_2	113.0	*f*
C35	113.8	*i*	Q63	122.3	4.6	E103*	117.9	6.5
K36	120.7	*h*	Q63 NH_2	111.4	*f*	E103	118.0	7.1
M37	116.2	5.1	D64	118.2	6.0	L104	117.8	8.9
I38	115.8	8.1	V65	121.9	5.6	V105	123.4	5.8
N39	125.3	*g*	A66	120.2	4.7			
N39*	125.3	*e*	S67	111.5	5.0			

[a] Residues which give distinguishable NH or $C_\alpha H$ ^1H chemical shifts for the two forms of human thioredoxin are denoted with an asterisk (*) at the amino acid name for the resonance arising from the major N-terminal valine species. ^{15}N chemical shifts are reported with respect to external liquid NH_3. [b] Unassigned resonance. [c] Resonance not observable at 40 °C. [d] Proline residue has no NH proton and no $^3J_{HN\alpha}$ coupling. Hence, the ^{15}N chemical shift can only be assigned through the observation of $C_\alpha H(i-1)$–$^{15}N(i)$ scalar connectivities. These were not observed for Pro-75. [e] Cross-peak too weak to measure coupling. [f] NH_2 group, therefore, no $^3J_{HN\alpha}$ coupling to measure. [g] The coupling is too small to measure, probably less than 3.75 Hz. [h] $^3J_{HN\alpha}$ coupling impossible to measure due to overlap. [i] Splitting pattern uninterpretable, perhaps due to multiple conformations.

by the method described above. The beginnings and ends of β-strands are well-defined by the NOEs across the sheet, but the extent of α-helices is much less obvious. Although the coupling constants of turns and loops may cover a broad range of values, they are not usually as small as expected for an ideal α-helix (4–5 Hz). Therefore, using the NH(i)–NH(i+1,2,3,4), $C_\alpha H(i)$–NH(i+1,2,3,4), and $C_\alpha H(i)$–$C_\beta H(i+3)$ ^1H NOEs in conjunction with the $^3J_{HN\alpha}$ values derived from the HMQC–J spectrum, the four α-helices of human thioredoxin were reexamined to obtain a better definition of their starting and ending points. As a result, the previous placement of secondary structure elements was found to be essentially correct except for α_3, which seems to begin at Gln-63, rather than at Cys-62 as thought earlier, due to the very high $^3J_{HN\alpha}$ value of 9.9 Hz for this residue, which is inconsistent with helical structure.

In addition, an assessment of the degree to which both the α-helices and the β-strands of human thioredoxin maintain ideal geometry can be made. The β-strands β_1, β_2, β_3, and β_4 appear to be quite regular, with couplings ranging from 8 to 10 Hz. However, β_5, a strand at the edge of the sheet, deviates substantially from a completely extended chain. This is evident from both the pattern of NH(i)–NH(i+1) NOEs, which are not seen for an ideal β conformation, and the $^3J_{HN\alpha}$ values of 4.7, 6.2, and 5.6 Hz for residues Gly-87, Glu-88, and Phe-89, respectively, which correspond to backbone torsion angles more consistent with an irregular than an extended structure. A number of the α-helices in human thioredoxin contain distortions from ideal geometry as well. In α_2, which contains Pro-40, residue Ile-38 has a coupling of 8.1 Hz and Phe-41 has one of 6.5, both larger than expected within a perfect α-helical stretch. The end of this helix is also distorted with couplings of 7.2, 7.5, and 8.9 Hz for residues Glu-47, Lys-48, and Tyr-49, respectively. Similar effects are apparent at the ends of α_3 and α_4 which seem to exhibit conformations deviating from the ideal α-helical geometry, with Cys-69 and Glu-70 in α_3 having couplings of 8.5 and 6.9 Hz and residues Leu-104 and Val-105 in α_4 having couplings of 8.9 and 5.8 Hz. Thus, the accurate $^3J_{HN\alpha}$ values obtained from the

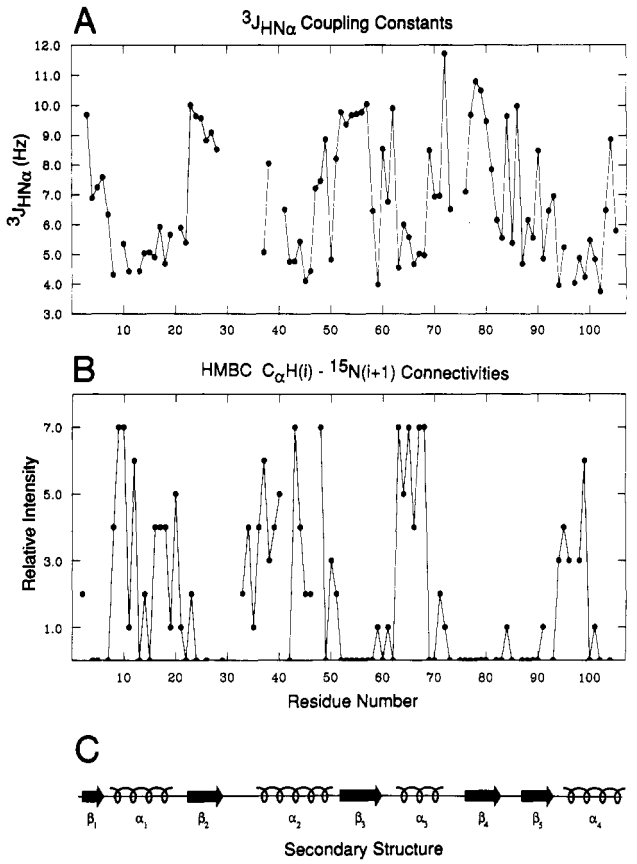

FIGURE 4: (A) $^3J_{HN\alpha}$ coupling constants for the residues of the major N-terminal Val species of reduced recombinant human thioredoxin, measured from the HMQC-J experiment and corrected to remove errors from dispersive components to the line shape and multiplet overlap effects. The reasons for the absence of several values in the figure is indicated in Table I. (B) Relative intensities of the scalar $C_\alpha H(i)$-$^{15}N(i+1)$ connectivities from the HMBC experiment, plotted as a function of residue number. Missing data represent unassigned connectivities due to overlapping or unidentified ^{15}N resonances. (C) Secondary structure of human thioredoxin determined from a qualitative analysis of ^1H NOE patterns and NH exchange data, provided as a reference to illustrate the correlation of these two NMR parameters with the secondary structure of the protein.

HMQC-J spectrum permit the secondary structure of human thioredoxin to be described more precisely than can be achieved on the basis of the data obtained from homonuclear experiments alone.

A second heteronuclear ^{15}N-^1H experiment was analyzed that also correlates well with the secondary structure of the protein. The HMBC experiment yields correlations between atoms separated by two and three bonds, including those to $C_\alpha H(i)$ from both $^{15}N(i)$ and $^{15}N(i+1)$. The presence of scalar $C_\alpha H(i)$-$^{15}N(i+1)$ connectivities confirms the sequential assignments. More importantly, the intensities of these connectivities, which are related to the ψ backbone torsion angle, also confirm the secondary structure determination. The magnitude of the $^3J_{N\alpha}$ coupling constant is related to the ψ angle via a Karplus-type relationship and has a maximum absolute value of 6 Hz for $\psi = -60°$. Couplings greater than 2 Hz arise for $-120° < \psi < 0°$, which overlaps the torsion-angle range found within α-helices, and couplings less than 2 Hz are seen for all other ψ values, including those found in β-strands (Bystrov, 1976). The intensity of the scalar $C_\alpha H(i)$-$^{15}N(i+1)$ cross-peak is strongly dependent on the size of the heteronuclear coupling, the transverse relaxation time, and the multiplicity of the ^1H multiplet (Clore et al., 1988). Considering that the ^1H T_2 values for a protein the size of thioredoxin are relatively short (<50 ms), couplings smaller than about 3 Hz are not expected to yield observable correlations. Consequently, $C_\alpha H(i)$-$^{15}N(i+1)$ cross-peaks are predicted to be observed principally in α-helical regions. This makes the HMBC experiment useful for confirming sequential assignments or determining them a priori within α-helical regions where the sequential $C_\alpha H(i)$-$NH(i+1)$ NOEs are weakest.

As expected from this analysis, the scalar $C_\alpha H(i)$-$^{15}N(i+1)$ cross-peaks are most apparent between residues Lys-8 and Lys-21, Pro-34 and Tyr-49, Gln-63 and Cys-69, and Lys-94 and Thr-100 of human thioredoxin, overlapping significant portions of α-helices α_1, α_2, α_3, and α_4, respectively. A summary of the relative intensities of the $C_\alpha H(i)$-$^{15}N(i+1)$ connectivities of the protein is presented in Figure 4B. The correlation between the magnitude of the HMBC peaks and secondary structure features is clearly demonstrated. Here again, irregularities within the secondary structure elements can easily be detected. For example, Phe-42, within helix α_2, exhibits a very weak $C_\alpha H(i)$-$^{15}N(i+1)$ connectivity, confirming the finding, based on $^3J_{HN\alpha}$ coupling constant analysis, of irregular geometry near Pro-40. Similar effects of nonideal conformations are found at the end of helix α_4.

Concluding Remarks

Two-dimensional heteronuclear ^{15}N-^1H NMR experiments on completely ^{15}N labeled proteins provide significant information relevant to a solution structure determination that can confirm and complement data extracted from homonuclear ^1H experiments. The HMQC, HMQC-NOESY, and HMQC-COSY experiments yield an independent check on the sequential proton resonance assignment, and the HMQC-NOESY permits the resolution of many ambiguities in long-range NOE assignments necessary to extract distance data for use in tertiary structure calculations. $^3J_{HN\alpha}$ coupling constants measured from the HMQC-J spectrum are more accurate, and the number of measurable couplings is greater than could be derived from homonuclear COSY-type spectra, particularly for a protein of the size of human thioredoxin and larger ones where broad NH line widths preclude the measurement of small couplings (Kay et al., 1989). The high level of confidence in the values for these couplings has led to a more precise determination of the secondary structure of human thioredoxin in terms of both the extents of the secondary structural elements and the degree to which they maintain ideal geometry. Finally, sequential scalar $C_\alpha H(i)$-$^{15}N(i+1)$ connectivities in the HMBC experiment allow confirmation of sequential assignments, particularly since the corresponding cross-peaks are strongest in α-helical regions where the homonuclear $C_\alpha H(i)$-$NH(i+1)$ NOE is weakest. Moreover, since the $^3J_{HN\alpha}$ values and the intensity of the HMBC $C_\alpha H(i)$-$^{15}N(i+1)$ peaks are related to the ϕ and ψ torsion angles of the peptide backbone, respectively, these parameters are invaluable to confirm the secondary structure obtained by homonuclear experiments alone and can be analyzed in their own right to determine the secondary structure. Thus, even in cases where the ^1H chemical shift dispersion is sufficient for assignment using only homonuclear methods, heteronuclear ^{15}N-^1H experiments can be extremely useful for larger proteins in providing additional data to be incorporated into a structural study of these macromolecules.

References

Bax, A., & Summers, M. F. (1986) *J. Am. Chem. Soc. 108*, 2093-2094.

Bax, A., & Marion, D. (1988) *J. Magn. Reson. 78*, 186-191.

Bax, A., Griffith, R., & Hawkins, B. L. (1983) *J. Magn. Reson. 55*, 301.
Bax, A., Kay, L. E., Sparks, S. W., & Torchia, D. A. (1989) *J. Am. Chem. Soc. 111*, 408.
Bendell, M. R., Pegg, D. T., & Doddrell, D. M. (1983) *J. Magn. Reson. 52*, 81.
Bystrov, V. F. (1976) *Prog. Nucl. Reson. Spectrosc. 10*, 41-81.
Clore, G. M., & Gronenborn, A. M. (1987) *Protein Eng. 1*, 275-288.
Clore, G. M., & Gronenborn, A. M. (1989) *CRC Crit. Rev. Biochem. Mol. Biol. 24*, 479-564.
Clore, G. M., Bax, A., Wingfield, P., & Gronenborn, A. M. (1988) *FEBS Lett. 238*, 17-21.
Forman-Kay, J. D., Clore, G. M., Driscoll, P. C., Wingfield, P., Richards, F. M., & Gronenborn, A. M. (1989) *Biochemistry 28*, 7088-7097.
Gronenborn, A. M., Bax, A., Wingfield, P. T., & Clore, G. M. (1989a) *FEBS Lett. 243*, 93-98.
Gronenborn, A. M., Wingfield, P. T., & Clore, G. M. (1989b) *Biochemistry 28*, 5081-5089.
Karplus, M. (1963) *J. Am. Chem. Soc. 85*, 2870.
Kay, L. E., & Bax, A. (1990) *J. Magn. Reson.* (in press).
Kay, L. E., Brooks, B., Sparks, S. W., Torchia, D. A., & Bax, A. (1989) *J. Am. Chem. Soc. 111*, 1515-1516.
Marion, D., & Wüthrich, K. (1983) *Biochem. Biophys. Res. Commun. 113*, 967-974.
Marion, D., Kay, L. E., Sparks, S. W., Torchia, D. A., & Bax, A. (1989a) *J. Am. Chem. Soc. 111*, 1515-1516.
Marion, D., Driscoll, P. C., Kay, L. E., Wingfield, P. T., Bax, A., Gronenborn, A. M., & Clore, G. M. (1989b) *Biochemistry 28*, 6150-6156.
Neuhaus, D., Wagner, G., Vasák, M., Kägi, J. H. R., & Wüthrich, K. (1985) *Eur. J. Biochem. 151*, 257-273.
Pardi, A., Billeter, M., & Wüthrich, K. (1984) *J. Mol. Biol. 180*, 741-751.
Powell, M. J. D. (1965) *Comput. J. 7*, 303-307.
Wollman, E. E., d'Auriol, L., Rimsky, L., Shaw, A., Jacquot, J.-P., Wingfield, P., Graber, P., Dessarps, F., Robin, P., Galibert, F., Bertoglio, J., & Fradelizi, D. (1988) *J. Biol. Chem. 263*, 15506-15512.
Wüthrich, K. (1986) *NMR of Proteins and Nucleic Acids*, Wiley, New York.
Zuiderweg, E. R. P., & Fesik, S. W. (1989) *Biochemistry 28*, 2387-2391.

Environments and Conformations of Tryptophan Side Chains of Gramicidin A in Phospholipid Bilayers Studied by Raman Spectroscopy†

Hideo Takeuchi, Yasuhisa Nemoto,‡ and Issei Harada*
Pharmaceutical Institute, Tohoku University, Aobayama, Sendai 980, Japan
Received July 12, 1989; Revised Manuscript Received October 9, 1989

ABSTRACT: Raman spectroscopy has been used to investigate the hydrophobic interaction of the indole ring with the environments, the water accessibility to the N_1H site, and the conformation about the C_β–C_3 bond for the four tryptophan side chains of gramicidin A incorporated into phospholipid bilayers. Most of the tryptophan side chains of the head-to-head helical dimer transmembrane channel are strongly interacting with the lipid hydrocarbon chains, and the hydrophobic interactions for the rest increase with increasing hydrocarbon chain length of the lipid. One tryptophan side chain (probably Trp-15) is accessible to water molecules, another (Trp-9) is deeply buried in the bilayer and inaccessible, and the accessibilities of the remaining two (Trp-11 and Trp-13) depend on the bilayer thickness. The torsional angle about the C_β–C_3 bond is found to be ±90° for all the tryptophans irrespective of the membrane thickness. Binding of the sodium cation to the channel does not change the torsional angles but decreases the water accessibilities of two tryptophans (Trp-11 and Trp-13) considerably. In conjunction with a slight spectral change in the amide III region, it is suggested that the sodium binding causes a partial change in the main-chain conformation around Trp-11 and Trp-13, which results in the movements of these side chains toward the bilayer center. Two models consistent with the present Raman data are proposed for the tryptophan orientation in the dominant channel structure.

Gramicidin A is a linear pentadecapeptide composed of alternating L- and D-amino acids with the N- and C-terminal residues blocked by a formyl and an ethanolamide group, respectively: HCO-L-Val-Gly-L-Ala-D-Leu-L-Ala-D-Val-L-Val-D-Val-L-Trp-D-Leu-L-Trp-D-Leu-L-Trp-D-Leu-L-Trp-$NHCH_2CH_2OH$ (Sarges & Witkop, 1964). This peptide forms transmembrane channels that induce permeability to monovalent cations and water in natural and artificial lipid membranes (Hladky & Haydon, 1972; Myers & Haydon, 1972; Rosenberg & Finkelstein, 1978; Finkelstein & Andersen, 1981). The structure of the channel has been studied extensively by various physicochemical methods, and a model proposed by Urry (1971) for the backbone conformation is now generally accepted (Weinstein et al., 1980; Urry et al., 1982b, 1983; Wallace et al., 1986). According to the model, the channel is a dimer consisting of two left-handed β-helical

†Supported in part by a Grant-in-Aid for General Scientific Research (62570958) from the Ministry of Education, Science and Culture of Japan.
‡Present address: Department of Cell Biology, The Research Institute for Tuberculosis and Cancer, Tohoku University, Seiryo, Aoba, Sendai 980, Japan

0006-2960/90/0429-1572$02.50/0